Heat transfer of thin-film Casson hybrid nanofluid flow across an unsteady stretching sheet

Nur Ilyana Kamis[a,1], Md Faisal Md Basir [a,2,*], Taufiq Khairi Ahmad [a,3], Lim Yeou Jiann [a,4]

[a] Department of Mathematical Sciences, Faculty of Science, Universiti Teknologi Malaysia, 81310 UTM Johor Bahru, Malaysia
[1] mfaisalmbasir@utm.my*
* corresponding author

ARTICLE INFO

Keywords
Thin-film
Suction
Nanoparticles;
Keller-box method

ABSTRACT

Hybrid nanoparticles copper and alumina effect on the heat transfer of thin-film blood flow toward an unsteady permeable stretching sheet is studied. The influence of suction is considered. The governing partial differential equations together with boundary conditions are reduced into the set of ordinary differential equations by implementing the similarity transformations. The Keller-box method is used to solve the momentum and heat equations. The characteristics of the blood flow and heat transfer under the effect of unsteadiness parameter, nanoparticles volume fraction, Casson parameter, and intensity of suction for different thin-film thickness are discussed. The numerical results of the velocity and temperature profiles are graphically displayed. The physical interest such as the local skin friction and Nusselt number are depicted in a tabular form.

1. Introduction

The improvement of innovations these days makes the laminar thin-film flow over a stretching sheet possible. The thin-film flow likewise has a significant capacity in numerous mechanical applications. For example, slim film sun-oriented cells, thin-film batteries, and dainty film photovoltaic cells. This has attracted the attention of numerous researchers to numerically or experimentally explore the behavior of the thin-film fluid flow and the heat transfer, for example [1]. These studies are important due to their massive potential to be utilized as a mechanical instrument in many designing applications. The principle utilization of such fluid is in coating processes, for example, in wire and fiber coatings. Based on the theory of thin-film flow indicated a common thin-film stream comprises a field of fluid mostly limited by a strong substrate with a (free) surface where the fluid is presented to another fluid [2]. The thickness one way is a lot more modest than the qualities length scale that other way. The stream happens transcendently toward one of the more drawn out measurements under the action of the external forces including gravity, surface pressure inclinations, and pivoting substrate.

The best nature of the coating cycle is controlled by the heat transfer when a sheet is stretched [3]. The first problem of this phenomenon has been explored by [4]. The issue in thin-film flow due to motivation by the research that has been, who have theoretically

analyzed the heat transfer and fluid flow along with a stretching sheet [5]. The development of non-Newtonian thin-film flow has been contributed by the following literature [6-9]. Cross-examined the MHD Casson fluid in a liquid film but the influence of viscous dissipation and internal heating has been elucidated [10]. An excellent performance between the analytical method and numerical method for solving the Casson fluid film has been reported together with slip and suction/injection effects in uniform film thickness when the sheet is stretched [11]. added the nanoparticles to the magneto-bioconvection of Casson fluid in a thin film over a similar geometry. The behavior of Casson fluid over a sheet that has been stretched was numerically studied [12].

On the other hand, the existence of nanoparticles in the fluid has affected the heat transfer in the fluid. The mixed nanoparticles, which are known as hybrid nanoparticles, will improve the heat transfer as contrasted with regular fluids [13]. The effect of the presence of hybrid nanoparticles on the heat transfer of the fluid [14],[15]. The perfect combination of various nanoparticle properties has demonstrated an outstanding heat transfer coefficient enhancement with a low-pressure decrease limit. Investigated the hybrid nanofluid and observed that the heat flux of the fluid is enhanced by the existence of the nanoparticles [16]. The free convection heat embedded with the hybrid nanofluid flow has been numerically explored[17]. Further, the increase of the material industrial productions has attracted the researcher to acknowledge and study the heat transfer in non-Newtonian fluids with nanoparticles. This is essential because in many practical applications the fluids involved are non-Newtonian and better thermal properties of the fluid are needed for heat transfer. The empirical and theoretical analysis of the Casson fluid with the inclusion of nanoparticles [18]. The enhancement of the temperature distribution in Casson fluid is due to elevating the volume fraction of nanoparticles in the fluid. The incrementation of the Casson fluid parameter also uplifts the velocity and temperature profiles as well as skin friction in a porous medium [19].

From the above mentioned literature, the investigation of hybrid nanoparticles and suction in a thin-film of Casson fluid through an unsteady stretching sheet has not been studied yet by any researchers. Thusly, this is the fundamental focal point of the current work. The PDEs form of governing equations will be transformed into the simple set of ODEs by employing the similarity transformations technique. Then, the Keller-Box method will be utilized to solve the similarity momentum and energy equations. The effect of the embedding parameters on velocity and temperature distributions will be discussed and illustrated graphically.

2. Method

This study considered an unsteady two-dimensional incompressible Casson fluid flow in a thin film. The film has a uniform thickness $h(t)$ as displays in Figure 1 [20]. The plane elastic sheet starts from a narrow slit wherein placed along $x-$axis as well as $y-$axis is perpendicular to it. The plane is stretching with velocity $U_w(x,t)=bx(1-\alpha t)^{-1}$. The constants appearing in the stretched rate are $b>0$ and $\alpha>0$. The fluid is being sucked, $V_w>0$ and injected, $V_w<0$ at the boundary layer with velocity $V_w=(V_w)_0(1-\alpha t)^{-0.5}$ where $(V_w)_0$ is an initial concentration of the reactant. The slit temperature, T_0 and reference temperature, T_{ref} at $y=0$ can be defined as $T_w(x,t)=T_0+T_{ref}\left[\frac{bx^2}{2\nu}\right](1-\alpha t)^{-1.5}$.

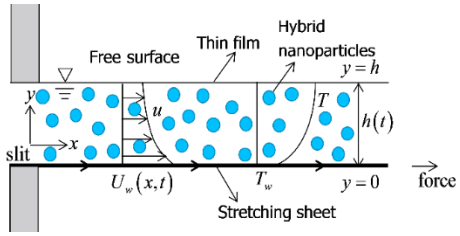

Fig. 1. Physical diagram

The rheological logical equation of state for an incompressible and isotropic flow of a non-Newtonian Casson fluid can be defined as [21],

$$\tau_{ij} = \begin{cases} 2\left(\mu_B + \dfrac{p_y}{\sqrt{2\pi}}\right)e_{ij}, \pi > \pi_e \\ 2\left(\mu_B + \dfrac{p_y}{\sqrt{2\pi_e}}\right)e_{ij}, \pi < \pi_e \end{cases}$$

Where μ_B is the plastic dynamic viscosity on the Casson fluid, the yield stress of fluid is P_y, π represent the product of the component of deformation rate with itself, namely, $\pi = e_{ij}e_{ij}, e_{ij}$ is the (i, j) component of the deformation rate and π_e is the critical values of π based on the Casson mode [22].

$$u_x + u_y = 0, \tag{1}$$

$$\rho_{hnf}\left(u_t + uu_x + vu_y\right) = \mu_{hnf}\left[1 + \frac{1}{\beta}\right]u_{yy}, \tag{2}$$

$$\left(\rho c_p\right)_{hnf}\left(T_t + uT_x + vT_y\right) = k_{hnf}T_{yy}. \tag{3}$$

where velocity segments along x and y direction is (u,v). k_{hnf} represents the conduction by the heat of nanodispersion, the density for the hybrid nanofluids is ρ_{hnf}, $\left(c_p\right)_{hnf}$ indicates the energy capacity of nanodispersion and μ_{hnf} demonstrates an effective dynamic viscosity and β is Casson fluid parameter. This is subjected to

$$y = 0;\ u = U_w,\ v = V_w,\ T = T_w, \tag{4}$$

$$y = h(t);\ \frac{\partial u}{\partial y} = \frac{\partial T}{\partial y} = 0,\ v = \frac{dh}{dt}. \tag{5}$$

where U_w and T_w denote the velocity and temperature. Introducing the following transformations vector $f(\eta)$ and $\theta(\eta)$,

$$\psi = \left[vb(1-\alpha t)^{-1}\right]^{\frac{1}{2}} x\delta f(\eta), \tag{6}$$

$$T = T_0 - T_{ref}\left(\frac{bx^2}{2\nu}\right)(1-\alpha t)^{-\frac{3}{2}}\theta(\eta), \tag{7}$$

$$\eta = \left(\frac{b}{\nu}\right)^{\frac{1}{2}}(1-\alpha t)^{-\frac{1}{2}}\delta^{-1}y. \tag{8}$$

Also, ϕ_1 and ϕ_2 are the volume fraction of alumina and copper. The characteristics of the hybrid nanofluids, copper and alumina as well as blood as base fluids are depicted in Table 1.

Table 1. Thermophysical properties of the fluid

Physical property	Blood	Alumina	Copper
$C_\rho\left(J/kgK\right)$	3617	765	385
$\rho\left(kg/m^3\right)$	1150	3970	8933
$k\left(W/mK\right)$	0.53	40	400

It is important to derivate the physical quantities of the fluid flow behavior that can be a good reference to researchers or engineers in practical applications. In this research, the physical quantities are the local skin fraction, C_f which depicts the wall shear stress, $\tau_w(x)$ and heat transfer rate $q_w(x)$ that is shown through the Nusselt number, Nu_x.

2.1 Numerical Method

The ODEs, Eqs (11) and (12) with the boundary conditions, Eqs (13) and (14) are solved by using the Keller-box technique. The details of the method can be found in the monograph [23]. The Keller box method that implements the finite difference method (FDM) is extremely powerful to get the numerical results to an arrangement of a nonlinear differential system. The four fundamental advances to get the mathematical arrangements through the Keller-box technique are:

- Reduce the governing equations into a system of first-order equations;
- The first-order system is written as a finite difference formula by applying the central differences formula;
- Linearize the subsequent equations by using the Newton technique and then, utilized on the coefficient of a matrix of the finite difference equations;
- The obtained linear system is understood utilizing the block elimination method by employing a block-tridiagonal factorization scheme.

Excellent preliminary guess with a uniform step size $\Delta h = 0.001$. Then, the Prandtl number for blood, $\mathrm{Pr} = 30$, has been fixed throughout the computational process with convergence criterion 10^{-5} is used to attain the solutions [24].

3. Result and Discussion

The behavior of the hybrid Casson nanofluid flow and heat transfer in a thin-film is separated into two cases; $\lambda = 1$ (thin) and $\lambda = 5$ (thick) of the thin film thickness through a permeable medium when the sheet is stretching. The numerical solutions are obtained for

various physical parameters values to explain in-depth the pattern of the physical problems [25] . Approval of the mathematical code is seen by looking at the mathematical consequences of the current examination, which solved the problem using HAM [26-30]. Table 2 provides a comparison of the numerical findings with previous publications in the absence of nanoparticles volume fraction $\phi_1 = \phi_2 = 0$, Casson parameter $\beta \to \infty$, suction parameter $w = 0$, and unsteadiness parameter $S = 0.8$ and $S = 1.2$ for different values of Prandtl number and it noticed that the current outcomes are discovered to be in amazing concurrence with distributed outcomes.

Table 2. Comparison of when and for different

	$\theta(\eta)$			
	$S = 0.8$		$S = 1.2$	
Pr	**Chun Wang (2006) [31]**	**Present study**	**Chun Wang (2006) [31]**	**Present study**
0.01	-0.0905	-0.0905	-0.0377	-0.0377
0.1	-0.7562	-0.7562	-0.3439	-0.3439
1	-3.5960	-3.5956	-1.9996	-1.9994
2	-5.2442	-5.2583	-2.9755	-2.9755

Table 3. Values of local skin friction $f''(0)$ and Nusselt number $\theta'(0)$ against the governing parameters, $S, \phi_1, \phi_2, \beta, w$

S	ϕ_1	ϕ_2	β	w	$f''(0)$		$\theta'(0)$	
					$\lambda = 1$	$\lambda = 5$	$\lambda = 1$	$\lambda = 5$
0.1					-	-	-15.9879	-63.9891
0.6					-0.5649	-2.0810	-16.5724	-65.0899
0.8					-0.6204	-2.2047	-	-
1.1					-0.6991	-2.3684	-17.1414	-65.9040
1.8					-0.8643	-2.6834	-17.9122	-67.0331
	0.01	0.01			-0.8696	-2.6657	-20.7709	-79.2143
	0.02	0.01			-0.8691	-2.6644	-20.2965	-77.0677
	0.03	0.01			-0.8680	-2.6617	-19.8383	-75.0007
	0.04	0.01			-0.8664	-2.6575	-19.3955	-73.0090
	0.01	0.02			-0.8970	-2.7354	-20.2957	-77.0727
	0.01	0.03			-0.9220	-2.7990	-19.8370	-75.0115
	0.01	0.04			-0.9448	-2.8570	-19.3940	-73.0263
			0.3		-0.6163	-2.0146	-18.1563	-67.3946
			0.6		-0.9075	-2.7619	-18.1270	-67.3529
			1.5		-1.2862	-3.7359	-18.0890	-67.2996
			10^8		-1.8316	-5.2260	-18.0353	-67.2201
				0.1	-0.6163	-2.0145	-18.1563	-67.3946
				0.2	-0.9075	-2.7619	-18.1270	-67.3529
				0.3	-1.2862	-3.7359	-18.0890	-67.2996
				0.4	-1.8316	-5.2260	-18.0353	-67.2200

Table 3 illustrates the detailed picture of local skin friction, $f''(0)$ and Nusselt number, $\theta'(0)$ for various values of pertinent parameters in a thinner and thicker thin-film thickness at the horizontal plate. Both values of local skin friction and Nusselt number for $\lambda = 1$ is higher than $\lambda = 5$ as elevating the values of all governing parameters. The physical reason behind these trends is that the uplifting of the thin-film thickness, λ promotes the resistance force to the fluid and then, tends to reduce the velocity of the motion of the particles along with the stretching sheet. Also, an incrementation of the thin film thickness additionally prompts an upgrade of the thickness of the fluid in the thin-film that causes

the raising of the viscosity. It is hard to improve the speed of viscous non-Newtonian fluid since more warmth is expected to beat the cohesive and adhesive forces of the fluid.

Based on Table 1, the increasing of unsteadiness parameter, S and suction parameter, w leads to enhance the values of local skin friction and Nusselt number. Therefore, the growth of these parameters, S and w cause an escalation in the wall shear stress and the heat transfer rate along with the stretching sheet. It is noticeable that the wall shear stress and heat flux enhance with increases in ϕ_1 although inequality of thin-film thickness [32-34]. At last, it is seen from a similar table that the frictional drag shows up from values of the local skin friction stifles and the rate of heat transfer described by the Nusselt number augments as the incrementation of ϕ_2 which showed the concentration of copper nanoparticles. The same behavior is demonstrated for the Casson parameter, β .

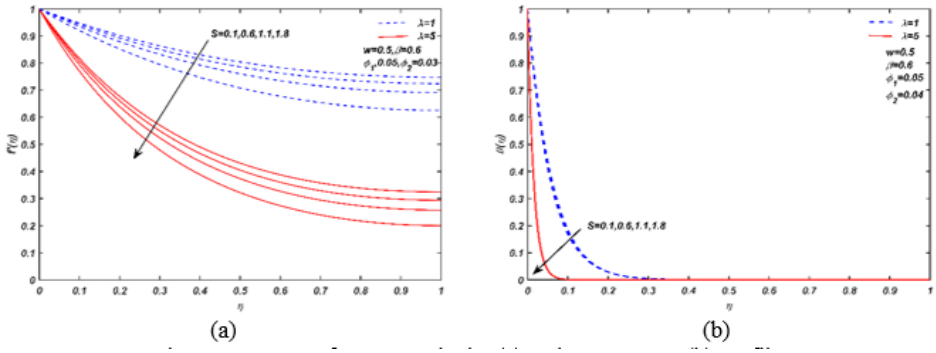

Fig. 2. Impact of over velocity (a) and temperature (b) profiles

Figures 2a and 2b unveil the patterns of velocity and temperature field for the growth of S . It is observed that both velocity and temperature profiles upsurge for increasing the values of S . The explanation for this phenomenon is that the enhancing parameter S , leads to a decline in the stretching rate at a horizontal plane of the film. Therefore, the movement of the particle in the fluid is stunted and more energy is required to improve the heat transfer in the thin-film. The momentum and thermal boundary layer decrease intensively. It is also found that from this Figure 2a and 2b, the particle moves faster with a high temperature in thinner of the thin film thickness, $\lambda = 1$ when compared with $\lambda = 5$.

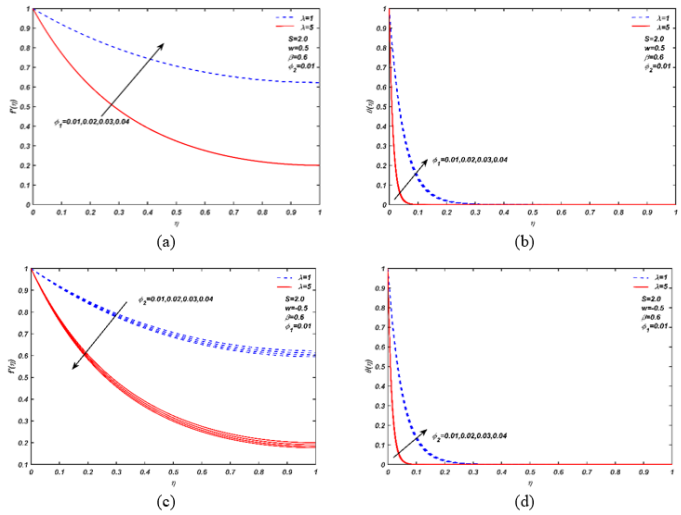

Fig. 3. Impact of ϕ_1 and ϕ_2 over velocity (a and c) and temperature (b and d) profiles

The variation of velocity and temperature profile for various concentration volume fraction nanoparticles copper ϕ_1 and alumina ϕ_2 when $\lambda = 1$ and $\lambda = 5$ are illustrated in Figures 3a, 3b, 3c and 3d. As the concentrations of alumina nanoparticles are more concentrated in the hybrid nanofluid film, the fluid flow is faster and the velocity is higher occur compared to enhance the concentrations of copper nanoparticles. The momentum boundary layer becomes thinner for increasing the ϕ_1 and ϕ_2. Considering that the density of copper is superior to alumina, thus, the pressure and force in the fluid become diminish.

The fluid moves gradually because of the lack of such force. However, the thermal boundary layer for both investigated parameters, ϕ_1 and ϕ_2 demonstrate similar trends. The incrementation of the nanoparticles upsurging the thermal conductivity in the fluid thereby more amount of heat in the fluid film when the sheet is stretched. Then, the nanoparticles scatter energy as warmth. In this way, more energy will be utilized when the expansion of nanoparticles in the fluid and simultaneously causes an increment in temperature and thickness of the thermal boundary layer. It can be is easily realized that the velocity of a fluid in a thin film is faster when the fluid contains a more concentrated alumina concentration. But the movement of the liquid is very weak in a thick film while containing a diluted concentration of alumina. The thinner thickness of the thin film stores more energy to aid fluid movement thus accelerating the fluid flow without relying on the concentration nanoparticles volume fraction when the sheet is stretching.

Figures 4a and 4b elucidate the effect of the Casson parameter β against the velocity and temperature field in a difference of thin-film thickness. Here, this study cross examined the values of β in the range of $0.3 \le \beta \le 10^8$. From the definition of the non-Newtonian Casson parameter, an increase in the values of β gives the lessening in the yield stress of the fluid and at the same time corresponds to enhance the plastic dynamic viscosity. In this case, the fluid behaves like a Newtonian fluid. Boosting the viscosity that induces resistance in the motion of the fluid molecules, which is capable of reducing the velocity in the film fluid. Thus, as β ascending to the higher values, the momentum boundary layer thickness squeezes steadily. Subsequently, an enriches in the Casson parameter prompts to uplift the temperature profile and their associated thermal boundary layer thickness intensifies. It is detected that the larger values of β gave a more prominent effect on the dimensionless velocity profile. From this Figure 4a, the fluid moves more casually at a thicker film thickness and activate an inferior amount of heat in the fluid than with a thin-film thickness.

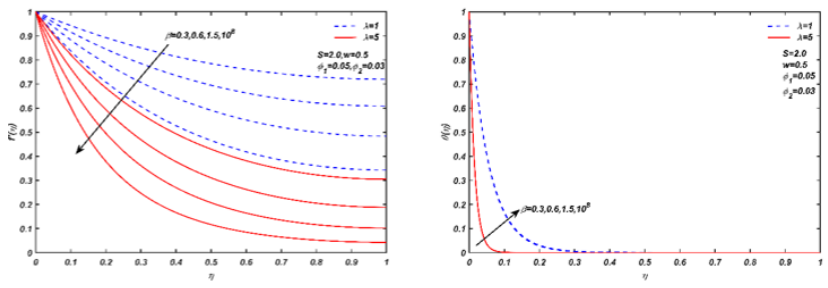

Fig. 4. Impact of β over velocity (a) and temperature (b) profiles

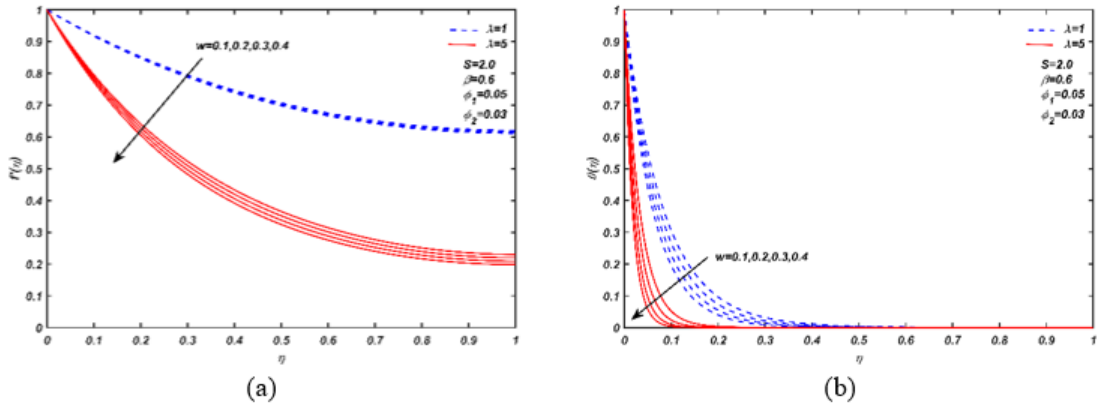

Fig. 5. Impact of w over velocity (a) and temperature (b) profiles

The effect of suction on dimensionless velocity and temperature profile reveal in Figure 5a and 5b, respectively. The movement of the fluid changes to a vacant in the film due to an increase in the value of w which in turn gives the effect of a change in the boundary layer. Hence, the velocity gets decelerated since the slow down of the molecules in the fluid regime and thereby curtailing the momentum boundary layer. It is impressing to note that the temperature distribution clarifies the look-alike as a velocity profile which is disclosed in Figure 5b. The reason behind this is that the upsurge in the suction attracts the number of fluids particles into the wall then reduces the thermal boundary layer of the fluid in the thin film. The diagram clearly demonstrates a very significant difference in the distribution of velocity and temperature depending on the thickness of the film. The thicker the thin film thickness, the faster the fluid flows along with the higher heat content in the fluid.

4. Conclusion

The target of this examination is to dissect the issue of Casson hybrid nanofluid in a thin film over an unsteady stretching sheet. The model is utilized along with the suction impact and hybrid nanoparticles. The transformed governing equations associated with mixed boundary conditions have been managed mathematical strategy specifically, the Keller box technique. The changing pattern of the local skin friction and Nusselt number for explored boundaries are introduced in tabular just as velocity and temperature fields graphically. Divergence of the thin-film thickness gave a pronounced effect on the parameter style investigated. The magnitude of the wall shear stress and Nusselt number, as well as velocity and temperature fields, are found to be diminished with the growth of the parameters and . The momentum and thermal boundary layer are noticed to enhance intensively together with the pattern of fluid movement and amount of heat in the fluid as the values of boots in the thin-film.

ACKNOWLEDGMENT

Special thanks to research grants vote 5F251 from the Ministry of Higher Education (MOHE) and vote 17J52 from the Research Management Center-UTM, Universiti Teknologi Malaysia (UTM) as our financial support.

References

[1] Abbas, Z., Sheikh, M., & Motsa, S. S. (2016). Numerical solution of binary chemical reaction on stagnation point flow of Casson fluid over a stretching/shrinking sheet with thermal radiation. *Energy, 95*, 12-20. doi:10.1016/j.energy.2015.11.039

[2] Ali, H. (2020). *Hybrid Nanofluids for Convection Heat Transfer*.

[3] Andersson, H., Aarseth, J., Braud, N., & Dandapat, B. (1996). Flow of a power-law fluid film on an unsteady stretching surface. *Journal of Non-Newtonian Fluid Mechanics, 62*(1), 1-8.

[4] Anitha, S., Thomas, T., Parthiban, V., & Pichumani, M. (2019). What dominates heat transfer performance of hybrid nanofluid in single pass shell and tube heat exchanger? *Advanced Powder Technology, 30*(12), 3107-3117. doi:https://doi.org/10.1016/j.apt.2019.09.018

[5] Bai, M.-j., Liu, J.-l., He, J., Li, Z.-y., Wei, J.-j., Chen, L.-x., Li, C.-m. (2020). High efficiency heat transfer and antifriction characteristics of SMWCNTs nanofluids. *Diamond and Related Materials, 105*, 107792. doi:https://doi.org/10.1016/j.diamond.2020.107792

[6] Carragher, P., & Crane, L. (1982). Heat transfer on a continuous stretching sheet. *ZAMM-Journal of Applied Mathematics and Mechanics/Zeitschrift für Angewandte Mathematik und Mechanik, 62*(10), 564-565.

[7] Cebeci, T., & Bradshaw, P. (1988). *Physical and computational aspects of convective heat transfer*. New York: Springer.

[8] Crane, L. J. (1970). Flow past a stretching plate. *Zeitschrift für angewandte Mathematik und Physik ZAMP, 21*(4), 645-647.

[9] El-Aziz, M. A., & Afify, A. A. (2016). Effects of Variable Thermal Conductivity with Thermal Radiation on MHD Flow and Heat Transfer of Casson Liquid Film Over an Unsteady Stretching Surface. *Brazilian Journal of Physics, 46*(5), 516-525. doi:10.1007/s13538-016-0442-3

[10] Hashimoto, S., Kurazono, K., & Yamauchi, T. (2020). Anomalous enhancement of convective heat transfer with dispersed SiO2 particles in ethylene glycol/water nanofluid. *International Journal of Heat and Mass Transfer, 150*, 119302. doi:https://doi.org/10.1016/j.ijheatmasstransfer.2019.119302

[11] Hussien, A., Md Yusop, N., Abdullah, M. Z., Al-Nimr, M., & Janvekar, A. A. (2017). *Heat Transfer Enhancement using Hybrid Nanofluids*.

[12] Izadi, M., Mohebbi, R., Karimi, D., & Sheremet, M. A. (2018). Numerical simulation of natural convection heat transfer inside a ⊥ shaped cavity filled by a MWCNT-Fe3O4/water hybrid nanofluids using LBM. *Chemical Engineering and Processing - Process Intensification, 125*, 56-66. doi:https://doi.org/10.1016/j.cep.2018.01.004

[13] Kamyar, A., Saidur, R., & Hasanuzzaman, M. (2012). Application of Computational Fluid Dynamics (CFD) for nanofluids. *International Journal of Heat and Mass Transfer, 55*(15), 4104-4115. doi:https://doi.org/10.1016/j.ijheatmasstransfer.2012.03.052

[14] Khan, N. S., Islam, S., Gul, T., Khan, I., Khan, W., & Ali, L. (2018). Thin film flow of a second grade fluid in a porous medium past a stretching sheet with heat transfer. *Alexandria Engineering Journal, 57*(2), 1019-1031. doi:https://doi.org/10.1016/j.aej.2017.01.036

[15] Mahmoud, M. A. A., & Megahed, A. M. (2017). MHD Flow and Heat Transfer Characteristics in a Casson Liquid Film Towards an Unsteady Stretching Sheet with Temperature-Dependent Thermal Conductivity. *Brazilian Journal of Physics, 47*(5), 512-523. doi:10.1007/s13538-017-0518-8

[16] Makinde, O. D., & Rundora, L. (2017). Unsteady mixed convection flow of a reactive casson fluid in a permeable wall channel filled with a porous medium. *Defect and Diffusion Forum, 377*, 166-179. doi:10.4028/www.scientific.net/DDF.377.166

[17] Megahed, A. (2015). Effect of slip velocity on Casson thin film flow and heat transfer due to unsteady stretching sheet in presence of variable heat flux and viscous dissipation. *Applied Mathematics and Mechanics, 36*(10), 1273-1284.

[18] O'Brien, S., & Schwartz, L. (2002). Theory and modeling of thin film flows. *Encyclopedia of Surface and Colloid Science*, 5283-5297.

[19] Raju, C. S. K., & Sandeep, N. (2017). Unsteady Casson nanofluid flow over a rotating cone in a rotating frame filled with ferrous nanoparticles: A numerical study. *Journal of Magnetism and Magnetic Materials*, *421*, 216-224. doi:10.1016/j.jmmm.2016.08.013

[20] Rawi, N. A., Ilias, M. R., Lim, Y. J., Isa, Z. M., & Shafie, S. (2017). *Unsteady mixed convection flow of Casson fluid past an inclined stretching sheet in the presence of nanoparticles.* Paper presented at the Journal of Physics: Conference Series.

[21] Ray Atul, K., Vasu, B., Anwar Beg, O., Gorla, R. S. R., & Murthy, P. V. S. N. (2019). Magneto-bioconvection flow of a casson thin film with nanoparticles over an unsteady stretching sheet: HAM and GDQ computation. *International Journal of Numerical Methods for Heat & Fluid Flow, 29*(11), 4277-4309. doi:10.1108/HFF-02-2019-0158

[22] Rehman, S., Idrees, M., Shah, R. A., & Khan, Z. (2019). Suction/injection effects on an unsteady MHD Casson thin film flow with slip and uniform thickness over a stretching sheet along variable flow properties. *Boundary Value Problems, 2019*(1), 26. doi:10.1186/s13661-019-1133-0

[23] Rehman, S., Shah, R. A., Khan, A., & Khan, Z. (2020). Free surface film flow of an unsteady second grade fluid over a stretching sheet with surface tension linearly varies with temperature. *Physica A: Statistical Mechanics and its Applications*, 123956. doi:https://doi.org/10.1016/j.physa.2019.123956

[24] Sakiadis, B. C. (1961). Boundary-layer behavior on continuous solid surfaces: II. The boundary layer on a continuous flat surface. *AIChE Journal*, *7*(2), 221-225. doi:10.1002/aic.690070211

[25] Samrat, S. P., Sulochana, C., & Ashwinkumar, G. P. (2019). Impact of Thermal Radiation on an Unsteady Casson Nanofluid Flow Over a Stretching Surface. *International Journal of Applied and Computational Mathematics*, *5*(2). doi:10.1007/s40819-019-0606-2

[26] Sulochana, C., Samrat, S. P., & Sandeep, N. (2018). Magnetohydrodynamic radiative liquid thin film flow of kerosene based nanofluid with the aligned magnetic field. *Alexandria Engineering Journal, 57*(4), 3009-3017. doi:https://doi.org/10.1016/j.aej.2017.11.005

[27] Vijaya, N., Sreelakshmi, K., & Sarojamma, G. (2016). Effect of magnetic field on the flow and heat transfer in a Casson thin film on an unsteady stretching surface in the presence of viscous and internal heating. *Open Journal of Fluid Dynamics*, *6*(4), 303-320.

[28] Waini, I., Ishak, A., & Pop, I. (2019). Unsteady flow and heat transfer past a stretching/shrinking sheet in a hybrid nanofluid. *International journal of heat and mass transfer*, *136*, 288-297. doi:https://doi.org/10.1016/j.ijheatmasstransfer.2019.02.101

[29] Waini, I., Ishak, A., & Pop, I. (2020). MHD flow and heat transfer of a hybrid nanofluid past a permeable stretching/shrinking wedge. *Applied Mathematics and Mechanics*, *41*(3), 507-520. doi:10.1007/s10483-020-2584-7

[30] Wang, C. (1990). Liquid film on an unsteady stretching surface. *Quarterly of Applied Mathematics, 48*(4), 601-610.

[31] Wang, C. (2006). Analytic solutions for a liquid film on an unsteady stretching surface. *Heat and Mass Transfer, 42*(8), 759-766.

[32] Yazid, M. N. A. W. M., Sidik, N. A. C., & Yahya, W. J. (2017). Heat and mass transfer characteristics of carbon nanotube nanofluids: A review. *Renewable and sustainable energy reviews, 80*, 914-941. doi:https://doi.org/10.1016/j.rser.2017.05.192

[33] Zakharov, M., & Sadovsky, M. (2013). The role of blood circulatory system in thermal regulation of *animals* explained by entropy production analysis.

[34] Zuhra, S., Khan, N. S., & Islam, S. (2018). Magnetohydrodynamic second-grade nanofluid flow containing nanoparticles and gyrotactic microorganisms. *Computational and Applied Mathematics, 37*(5), 6332-6358. doi:10.1007/s40314-018-0683-6